THROUGH THE WALL IMAGING (TWI) WITH VIRTUAL APERTURE RADAR

Ana Maria Azinheiro Catarino nº 98415

Instituto Superior Técnico
Av. Rovisco Pais, 1049-001 Lisboa, Portugal
<ana.maria.catarino@tecnico.ulisboa.pt>

Abstract - Through-the-Wall Imaging (TWI Radar) is an emerging field of research, with promising applications ranging from research and rescue, to health care and security, for detecting, locating and identifying targets behind opaque obstacles. Thus, the radar is a fundamental tool in this process, mainly due to its long wavelength, which allows the signal to pass through building materials. However, this capability has disadvantages, namely the multipath reflections that are caused by the environment, which can reduce its usefulness.
Currently, there are several methods for obtaining this radar image, which are addressed in this thesis. However, there are challenges, as not all of these methods have high accuracy and reduced data acquisition time. In this context, there is a need to optimize these methods, fulfilling the necessary and favorable requirements to obtain the image of these targets using the radar.
This work presents a proposal to use a virtual aperture radar (Virtual Aperture Radar - VAR) to obtain an image through the wall as well as the development of a method that estimates the position, thickness and electrical permittivity of the wall.

Index terms - **Through-the-Wall Imaging (TWI); Virtual Aperture Radar (VAR); Synthetic Aperture Radar (SAR); MIMO Radar**

I .INTRODUCTION

The concept of Through-the-Wall Imaging (TWI) has received a lot of attention in the literature in recent years. Despite this interest and evolution over the years, there are still few methods for determining the location of targets behind the wall and, as such, to help solve this problem, a new method is investigated, which consists in the use of aperture radar. virtual to obtain the image. Traditional imaging methods are based on the assumption that the media are homogeneous, which is not valid in the case of TWI. In fact, the refraction of electromagnetic waves between the front and back surface of the wall makes the propagation path not a straight line. Traditional imaging methods ignore the influence of the wall, so the image formed on targets behind the wall appears blurred and objects are displaced from their true positions, which degrades the radar's performance.
In order to get a good focus on targets behind the wall, the wall effect must be considered during image processing, so the physical parameters of the wall need to be known. Fortunately, the radar receives signals reflected not only by the targets, but also by the surrounding environment, in this case, the wall, which theoretically allows extracting information about it from the received echo. In TWI, it is necessary to know the wall parameters, such as thickness and electrical permittivity, to obtain good quality images. The electrical permittivity of a wall can be estimated from the echo reflected from the front surface of the wall. However, this approach requires accurate calibration; other methods of imaging through the wall require the determination of the refraction point, for the calculation of the propagation path between the emitting (and/or receiving) antenna and the target behind the wall.

This work proposes the following:

• Implementation of the VAR model of image through the wall;
• Development of a method to estimate the position, thickness and electrical permittivity of the wall;
• Obtaining an RPF (Reflection-Point Free) image through the wall;
• Experimental validation of the proposed method, by comparing numerical results.

II. REALISTIC MODEL USING VAR

In this chapter, the expected results based on a study carried out by T. Jin and A. Yarovoy [1] will be presented, and later preliminary results will be presented, namely the study of incident wave between three different media based on the Realistic Model with monostatic radar antenna and with bistatic radar antenna. These results were supported with the MATLAB program.

A. Image through the wall using VAR

As mentioned in the previous chapter, a realistic model of a through-wall imaging system requires knowledge of certain parameters of the wall. Furthermore, it should be noted that when the linear MIMO array is parallel to the wall, the wall position can be defined by the distance between the front surface of the wall and the linear MIMO array. The Fig.1 represents the TWR image geometry with MIMO matrix [1].

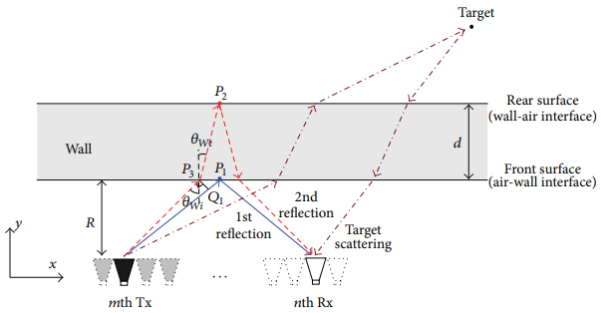

Fig.1- TWR image geometry with MIMO matrix [1]

As mentioned, [1], regarding the wall echo, the transmitted signal will be reflected on the front and rear surfaces of the wall. These reflections are denoted as 1st and 2nd reflections, respectively. The echo phase history of the 1st and 2nd reflections can be obtained from the electrical length of the bidirectional path traveled by a spherical wave from the transmit antenna to the reflection point and back to the receive antenna.

Given the *m*-th transmission element and the *n*th reception element located at $(x_{Tm},0)$ and $(x_{Rn},0)$, respectively, the elementary propagation path l_{W1} of the 1st reflection is

$$l_{W1} = 2r_{TxP1}, \tag{1}$$

where r_{TxP1} is the distance from the transmit antenna to the reflection point on the front surface P_1.

The propagation path of the 2nd reflection is the path through the air to the wall, followed by refraction from the front surface at P3 and reflection from the back surface at P2. The total equivalent propagation path l_{W2} in air is

$$l_{W2} = 2(r_{TxP3} + \sqrt{\varepsilon_r}\, r_{P3P2}), \tag{2}$$

where ε_r is the relative electrical permittivity of the wall and r_{TxP3} and r_{P3P2} are the distances from the transmit antenna to P3 and from P3 to P2, respectively.

When the transmission signal is refracted at point P3, the angle of incidence θ_{Wi} and the angle of refraction θ_{Wt} obey Snell's Law according to:

$$\frac{sin\theta_{Wi}}{\sin\,\theta_{Wt}} = \sqrt{\varepsilon_r}\,. \tag{3}$$

According to the geometry relationship represented in Fig. 1, one has to

$$\begin{aligned} r_{TxP3} &\approx r_{TxP1} - d\, tan\theta_{Wt} sin\theta_{Wi}, \\ r_{P3P2} &= \frac{d}{cos\theta_{Wt}}, \end{aligned} \tag{4}$$

where d is the wall thickness.

Substituting (4) into (2) and taking into account (3), we get

$$\begin{aligned} l_{W2} &= 2(r_{TxP1} + d\sqrt{\varepsilon_r - sin^2\theta_{Wi}}) \\ &= l_{W1} + 2d\sqrt{\varepsilon_r - sin^2\theta_{Wi}}. \end{aligned} \tag{5}$$

B. Estimation of wall parameters

The wall parameters through which the realistic model is characterized are the following: position, width and electrical permittivity, the same being estimated from the received echo.

As stated by Jin and Yarovoy [1], for the MIMO matrix, the time delay between the 1st reflection and the 2nd reflection with respect to the *m*-th transmitting element and the nth receiving element is:

$$t_d(m,n) = \frac{2d\sqrt{\varepsilon_r - sin^2\theta_{Wi}(m,n)}}{c} \tag{6}$$

$$\theta_{Wi}(m,n) \approx \arctan\left(\frac{|x_{Rn} - x_{Tm}|}{2R}\right), \tag{7}$$

where R is the distance between the MIMO matrix and the front surface, which can be estimated as

$$\hat{R} = \frac{1}{2MN}\sum_{m=1}^{M}\sum_{n=1}^{N}\sqrt{c^2 t_f^2(m,n) - (x_{Rn} - x_{Tm})^2}, \tag{8}$$

Where $t_f(m,n)$ is the time delay of the 1st reflection with respect to the *m*-th transmit antenna and *n*-th receiver antenna. The spatial resolution $\rho_r = c/(2B)$ is determined by the bandwidth of system B, where c is the speed of propagation of the EM wave in free space. According to the geometry, when the system bandwidth meets the condition

$$B = \frac{c\,\cos\theta_{Wt}}{2d\sqrt{\varepsilon_r}}, \tag{9}$$

reflections on the front and back surfaces of the wall can be separated on the baseband (or fast time). The relative electrical permittivity of unstressed concrete is contained in the band 5 to 9, depending on the relative humidity rate. Assuming ε_r = 6 and d = 0.2 m, it results from equation (9) that B > 307 MHZ for any refraction angle, which is generally met for most TWI radars.

Based on (6), (7) and (8), it has been

$$0.25c^2 t_d^2(m,n) = d^2\varepsilon_r - d^2\frac{(x_{Rn} - x_{Tm})^2}{(x_{Rn} - x_{Tm})^2 + 4\hat{R}^2} \tag{10}$$

which can be written in matrix form as

$$\mathbf{Ap = b} \tag{11}$$

With

$$\begin{aligned} \boldsymbol{A} &= \begin{bmatrix} 1 & -\frac{(x_{R1}-x_{T1})^2}{(x_{R1}-x_{T1})^2+4\hat{R}^2} \\ 1 & -\frac{(x_{R2}-x_{T1})^2}{(x_{R2}-x_{T1})^2+4\hat{R}^2} \\ & \vdots \\ 1 & -\frac{(x_{RN}-x_{TM})^2}{(x_{RN}-x_{TM})^2+4\hat{R}^2} \end{bmatrix}_{MN\times 2}, \\ \boldsymbol{p} &= \begin{bmatrix} d^2\varepsilon_r \\ d^2 \end{bmatrix} = \begin{bmatrix} p_1 \\ p_2 \end{bmatrix}, \\ \boldsymbol{b} &= \begin{bmatrix} 0.25c^2 t_d^2(1,1) \\ 0.25c^2 t_d^2(1,2) \\ \vdots \\ 0.25c^2 t_d^2(M,N) \end{bmatrix}_{MN\times 1}, \end{aligned} \tag{12}$$

The solution of (11) is

$$p = (\boldsymbol{A}^T\boldsymbol{A})^{-1}\boldsymbol{A}^T\boldsymbol{b}, \tag{13}$$

where the superscript $(.)^T$ is the transposition operator.

Width and relative electrical permittivity estimates are obtained according to

$$\begin{aligned}\hat{d} &= \sqrt{p_2},\\ \hat{\varepsilon_r} &= \frac{p_1}{p_2}.\end{aligned} \tag{14}$$

C. RPF penetrating imaging

It is known that the electrical equivalent length is independent of the distance between the radar and the air-wall interface, so it can be calculated using the geometry of Fig. 2. In turn, the MIMO matrix is defined on the front surface and P4 is the equivalent refraction point on the back surface. θ_{Ti} and θ_{Tt} are the incident and refraction angles, respectively, which obey the following relationship (Snell's law) [8],

$$\frac{\sin\theta_{Ti}}{\sin\theta_{Tt}} = \sqrt{\varepsilon_r}. \tag{15}$$

Therefore, the equivalent electrical length in air from the transmit antenna to the target can be expressed as

$$l_{TxTar} = (r_{TxP_4}\sqrt{\varepsilon_r} + r_{P_4Tar}), \tag{16}$$

where r_{TxP_4} and r_{P_4Tar} are the distances from the emitting antenna to the refraction point P4 and from the refraction point P4 to the target, respectively.
According to the geometric relationship described in Fig. 2, r_{TxP_4} and r_{P_4Tar} can be calculated through

$$\begin{aligned} r_{TxP_4} &= \frac{d}{\cos\theta_{Tt}},\\ r_{P_4Tar} &= r_{TxTar} - r_{P_4Q_2} = r_{TxTar} - \frac{d\cos(\theta_{Ti}-\theta_{Tt})}{\cos\theta_{Tt}},\\ &= r_{TxTar} - d(\cos\theta_{Ti} + \sin\theta_{Ti}\tan\theta_{Tt}), \end{aligned} \tag{17}$$

Where r_{TxTar} is the distance from the transmitting antenna to the target. Substituting (15), (17) into (16), l_{TxTar} can be rewritten as

$$l_{TxTar} = r_{TxTar} + d\left(\sqrt{\varepsilon_r - sin^2\theta_{Ti}} - \cos\theta_{Ti}\right). \tag{18}$$

Likewise, the equivalent electrical length in air from the target to the receiving element l_{TarRx} can be calculated as follows

$$l_{TarRx} = r_{TarRx} + d\left(\sqrt{\varepsilon_r - sin^2\theta_{Ri}} - \cos\theta_{Ri}\right). \tag{19}$$

When the target is located at a point *(x,y)* behind the wall, the delay time of its return with respect to the *m*th transmitting antenna and the *n*th receiving antenna can be estimated as

$$t_{T_1}(m,n) = \frac{\left[\sqrt{(x-x_{Tm})^2+(y-y_{Tm})^2} + \sqrt{(x-x_{Rn})^2+(y-y_{Rn})^2} + \hat{d}\right]}{\left(\sqrt{\hat{\varepsilon_r} - sin^2\theta_{Ti}(m,n)} - \cos\theta_{Ti}(m,n) + \sqrt{\hat{\varepsilon_r} - sin^2\theta_{Ri}(m,n)} - \cos\theta_{Ri}(m,n)\right)} \Big/ c \tag{20}$$

On what

$$\begin{aligned}\theta_{Ti}(m,n) &\approx arctan\left[\frac{(x-x_{Tm})}{(y-y_{Tm})}\right],\\ \theta_{Ri}(m,n) &\approx arctan\left[\frac{(x-x_{Rn})}{(y-y_{Rn})}\right].\end{aligned} \tag{21}$$

When the target is in front of the wall the delay of its return can be calculated as

$$t_{T_2}(m,n) = \frac{\left[\sqrt{(x-x_{Tm})^2+(y-y_{Tm})^2} + \sqrt{(x-x_{Rn})^2+(y-y_{Rn})^2}\right]}{c} \tag{22}$$

According to (20) and (22), the RPF penetrating imaging based on the realistic TWR model, is

$$I(x,y) = \begin{cases} \sum_{m=1}^{M}\sum_{n=1}^{N}\int s(t,m,n)\delta[t - t_{T_1}(m,n)]dt, & y \geq \hat{R} + 0.5\hat{d} \\ \sum_{m=1}^{M}\sum_{n=1}^{N}\int s(t,m,n)\delta[t - t_{T_2}(m,n)]dt, & y < \hat{R} + 0.5\hat{d}, \end{cases} \tag{23}$$

where $I(x,y)$ is the image formed, t is the fast time, and $s(t,m,n)$ is the received signal. It is understood that when the emitted signal is not a pulse but a frequency-scaled signal, $s(t,m,n)$ is the signal after compression and a phase compensation term must be added to (23) to ensure the phase coherence [1].

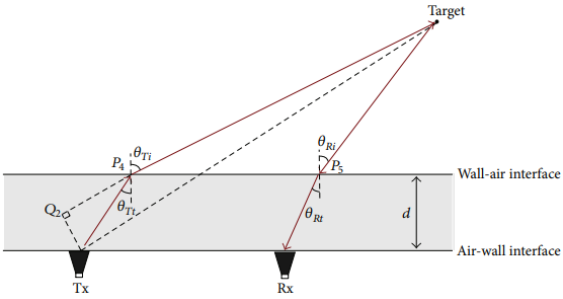

Fig.2-Equivalent two-layer propagation model [1]

D. Numerical simulations

D-1. Incident wave between three different media based on the Realistic Model with monostatic radar antenna

This subchapter presents an analytical and graphic study, approaching the realistic model.
This study is based on an incident wave between three middle, middle 1 and 3 which correspond to air and middle 2 which correspond to a masonry wall; in middle 3 there is a target at a distance of 30 cm, for example a person, with $\sigma = 1\ [m^2]$, so the radar antenna used will be of the monostatic type. Note that the middle parameters 1 and 3 (air) are as follows: $\sigma_{1/3} = 0\ [S.m^{-1}]$, $\varepsilon_{1/3} = \frac{10^{-9}}{36\pi}\ [F.m^{-1}]$, $\mu_{1/3} = 4\pi \times 10^{-7}\ [H.m^{-1}]$ and middle 2 are: $\sigma_2 = 0{,}005\ [S.m^{-1}]$, $\varepsilon_2 = 5{,}56\ [F.m^{-1}]$, $\mu_2 = 1\ [H.m^{-1}]$. And it is also known that $n_1 = 1$ and $n_2 = \sqrt{5{,}56}$. Next, the representative scheme of the incident wave based on the realistic model is presented.

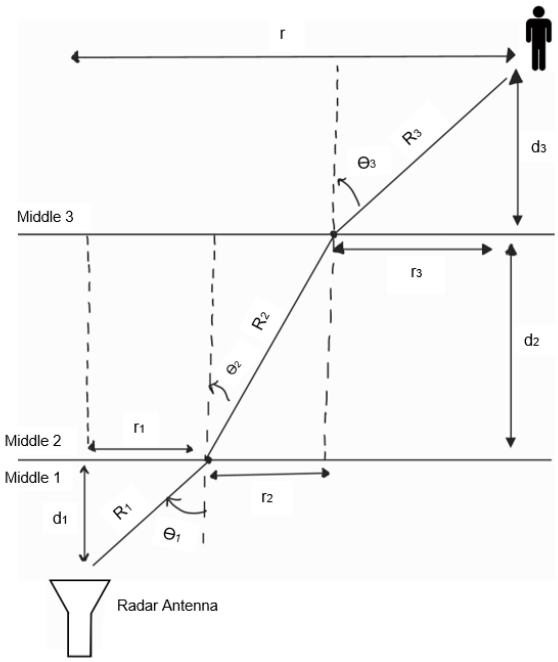

Fig.3- Representation of the angles and distances of an incident wave on air-wall-air using a monostatic radar antenna

Through observation of the figure, and application of the Snell-Descartes Law and consequent application of the Pythagorean theorem, by observation of the figure, the following expressions were obtained:

$$n_1 \sin\theta_1 = n_2 \sin\theta_2 \\ n_2 \sin\theta_2 = n_3 \sin\theta_3 \quad (24)$$

$$r = d_1 \tan\theta_1 + d_2 \tan\theta_2 + d_3 \tan\theta_3 \quad (25)$$

$$R = R_1 + R_2 + R_3 = \frac{d_1}{\cos\theta_1} + \frac{d_2}{\cos\theta_2} + \frac{d_3}{\cos\theta_3} \quad (26)$$

As verified in the previous subchapter, the horizontal polarization presented greater received power, so this type of polarization was used. We proceeded to the calculation of means 1-2, that is, in which we would have the term n_{12} , the calculation of the term n_{21}, as well as the calculation of the term n_{23} and the term n_{32}, this is done through the equation $n_{21} = \sqrt{\frac{\mu_2(\sigma_2 + jw\varepsilon_2)}{\mu_1(\sigma_1 + jw\varepsilon_1)}}$, making the necessary substitutions according to the intended means.
Thus, the following values were obtained:

$$n_{21} = n_{23} = 2{,}36 - 0{,}0019j \\ n_{12} = n_{32} = 0{,}42 + 3{,}477 \times 10^{-4} j$$

Knowing that $d_1 = 0{,}3m,\ d_2 = 0{,}15m\ and\ d_3 = 0{,}5m$ and a frequency of 1 GHz, we obtained a wall attenuation constant (α) of 0.127 Neper/m (equation (27) ($\gamma_{parede} = \alpha + j\beta = \sqrt{jw\mu(\sigma + jw\varepsilon)}$)).
Therefore, through the application of the radar equation of

$$P_r = \frac{P_e G^2 \lambda^2 \sigma}{(4\pi)^3 (R_1 + R_2 + R_3)^4} \times |T_{TM21}|^2 \times |T_{TM12}|^2 \\ \times |T_{TM23}|^2 \times |T_{TM32}|^2 e^{-4\alpha R_2} \quad (28)$$

The remaining parameters needed for the calculation were the following: received power (P_e) with a value of 5 Watts, receiving and transmitting antenna gain $G_r = G_e = G = 16$ dB = 31.6, a distance of 0.3 m, the cross section one-person radar (RCS), σ , which is assumed to be about 1 m^2 and a wavelength (λ) of 0.3 m.
Previously, a study was carried out based on the fact that the value of θ_1 is known, which is a fixed value, and θ_2 and θ_3 depend on it, where later it was possible to obtain the distance r (m), however this approach is not the most correct, because in a real scenario you will have to take into account the distance at which the radar antenna is placed and from this determine the angles of incidence. Having said that, a correction was made in the study carried out.
Thus, using the MATLAB program, the graphs were obtained that show the variation of the incidence angles θ_1 , θ_2 and θ_3 as a function of the distance r.

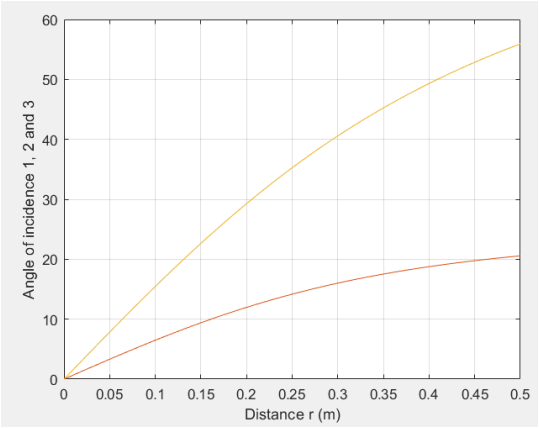

Fig.4 - Variation of angle values θ_1 (yellow), θ_2 (red) and θ_3 (yellow) as a function of distance r (m)

Therefore, the graph with the relationship of received power as a function of distance was obtained.

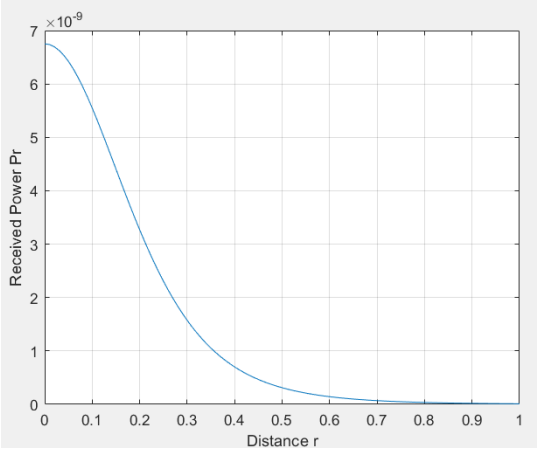

Fig.5 - Power received by the radar antenna as a function of distance r

D-2. Incident wave between three different media based on the Realistic Model with bistatic radar antennas

This subchapter presents an analytical and graphic study similar to the one carried out in the previous subchapter, however it differs in the fact that two radar antennas are used, but of the bistatic type, as outlined below.

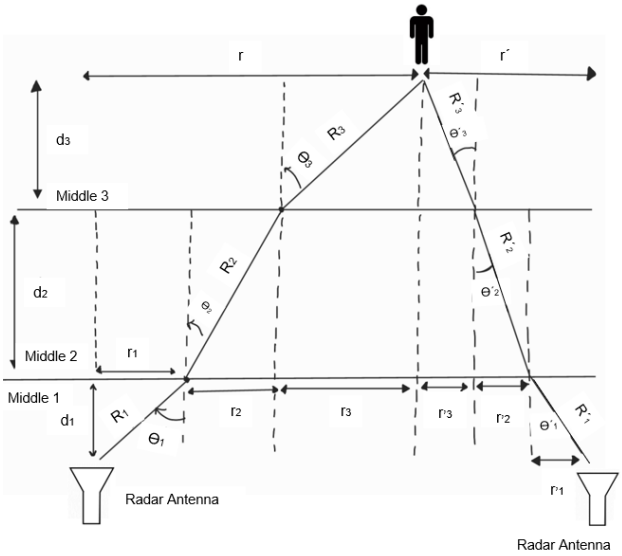

Fig.6 - Representation of angles and distances of an incident wave on air-wall-air using two bistatic radar antennas

Two different studies were carried out with this situation, the first where the distance from the target was known and the second study in which the distance to the target was unknown, these are presented below.
It should be noted that the polarization used was horizontal. As in the previous subchapter, the following terms were also used:

$$n_{21} = n_{23} = 2{,}36 - 0{,}0019j$$
$$n_{12} = n_{32} = 0{,}42 + 3{,}477 \times 10^{-4}j$$

D-2.1. Analytical study knowing how far away the target is from the wall

This study is based on an incident wave between three middle, middle 1 and 3 which correspond to air and middle 2 which correspond to a masonry wall, in which middle 2; in the middle 3 is a target at a distance of 30 cm, for example a person, with $\sigma = 1\ [m^2]$. Note that the middle parameters 1 and 3 (air) are as follows: $\sigma_{1/3} = 0\ [S.m^{-1}]$, $\varepsilon_{1/3} = \frac{10^{-9}}{36\pi}\ [F.m^{-1}]$, $\mu_{1/3} = 4\pi \times 10^{-7}\ [H.m^{-1}]$ and middle 2 are: $\sigma_2 = 0{,}005\ [S.m^{-1}]$, $\varepsilon_2 = 5{,}56\ [F.m^{-1}]$, $\mu_2 = 1\ [H.m^{-1}]$. It is also known that $n_1 = 1$ and $n_2 = \sqrt{5{,}56}$. The figure below illustrates the situation studied.
The radar equation was applied to obtain the received power as a function of distance, however it differs from the previous ones due to the fact that it has two bistatic radar antennas, being necessary to introduce the parameter R'_2 as can be seen from the expression below:

$$P_r = \frac{P_e G^2 \lambda^2 \sigma}{(4\pi)^3 (R_1 + R_2 + R_3)^2 (R'_1 + R'_2 + R'_3)^2} \times |T_{TM21}|^2 \times |T_{TM12}|^2 \times |T_{TM23}|^2 \times |T_{TM32}|^2 \times |T_{TM'21}|^2 \times |T_{TM'12}|^2 \times |T_{TM'23}|^2 \times |T_{TM'32}|^2 e^{-4\alpha R_2 R'_2} \quad (29)$$

As previously mentioned, this study was initially also approached according to a fixed incidence angle value θ_1, however this is not the most correct and real way of approaching the existing problem, so I will present the results according to the fixation of the value of the distance r and thus obtain the value of the angles of incidence.
To carry out this determination, the MATLAB program was used, in which the following expressions necessary to determine the incidence angles were used.

$$\begin{aligned} n_1 \sin\theta_1 &= n_2 \sin\theta_2 \\ n_2 \sin\theta_2 &= n_3 \sin\theta_3 \\ n_1 \sin\theta'_1 &= n_2 \sin{}'\theta'_2 \\ n_2 \sin\theta'_2 &= n_3 \sin\theta'_3 \end{aligned} \quad (30)$$

$$\begin{aligned} r &= d_1 \tan\theta_1 + d_2 \tan\theta_2 + d_3 \tan\theta_3 \\ r' &= d_1 \tan\theta'_1 + d_2 \tan\theta'_2 + d_3 \tan\theta'_3 \end{aligned} \quad (31)$$

It should be noted that $d_1 = 0{,}3m, d_2 = 0{,}15m$ and $d_3 = 0{,}5m$, $P_e = 50kw$ and a frequency of 1 GHz were used, resulting in a wall attenuation constant (α) of 0.127 Neper/m (equation (27)).
It should be noted that fixed values of r between 0 and 1 meter and distance between the antennas (D) of 2 meters were used, so r' will depend on these two parameters as follows:

$$D = r + r' \quad (32)$$

Thus, using the MATLAB program, the following graph was obtained, which represents the power received by both antennas as a function of the distance r.

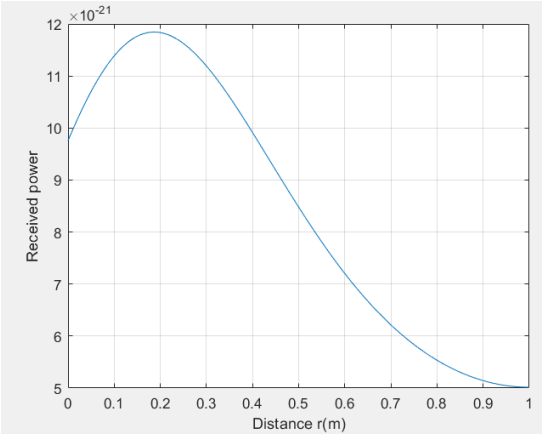

Fig.7 - Receiving power by the radar antenna as a function of distance

Using the MATLAB program, it was also possible to acquire the graph that represents the variation of the angle values $\theta_1, \theta_2, \theta_3$, θ'_1 , θ'_2 and θ'_3 as a function of the distance r (m), as can be seen in the figures below, respectively.

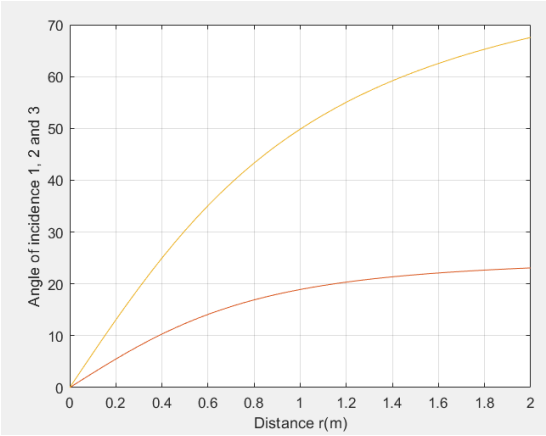

Fig.8 - Variation of the values of the angles of incidence θ_1, θ_2 and θ_3 as a function of the distance r (m)($\theta_1 = \theta_3$ which corresponds to the yellow curve and θ_2 red curve)

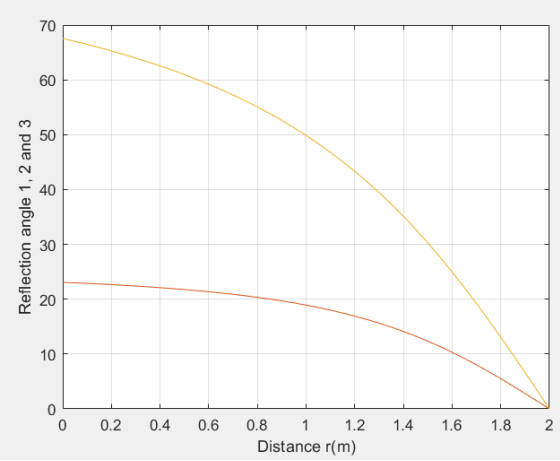

Fig.9 - Variation of the values of the reflection angles θ'_1, θ'_2 and θ'_3 as a function of the distance r (m) ($\theta'_1 = \theta'_3$ which corresponds to the yellow curve and θ'_2 red curve)

In turn, it was intended to carry out the same study but using the same previous antennas but with a pulsed radar, in order to calculate the total delay time.
To calculate the total delay time, the following expressions were used:

$$T_{total} = T_1 + T_2 + T_3 + T'_1 + T'_2 + T'_3 \quad (33)$$

Knowing that: $T_1 = \frac{R_1}{c_1}$, onde $R_1 = \frac{d_1}{\cos\theta_1}$ e $c_1 = c_0 = 3 \times 10^8\ m/s$.
$T_2 = \frac{R_2}{c_2}$, onde $R_2 = \frac{d_2}{\cos\theta_2}$ e $c_2 = \frac{c_0}{n_2}$
$T_3 = \frac{R_3}{c_3}$, onde $R_3 = \frac{d_3}{\cos\theta_3}$ e $c_3 = 3 \times 10^8\ m/s$.
$T'_1 = \frac{R'_1}{c_0}$, onde $R'_1 = \frac{d_1}{\cos\theta'_1}$ e $c_0 = 3 \times 10^8\ m/s$.
$T'_2 = \frac{R'_2}{c_2}$, onde $R'_2 = \frac{d_2}{\cos\theta'_2}$ e $c_2 = \frac{c_0}{n_2}$
$T'_3 = \frac{R'_3}{c_3}$, onde $R'_3 = \frac{d_3}{\cos\theta'_3}$ e $c_3 = 3 \times 10^8\ m/s$.

Subsequently, using the MATLAB program, the following graph was obtained, which represents the distance r as a function of the total delay time.

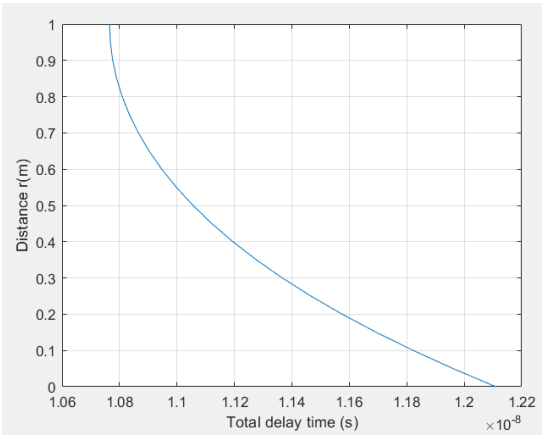

Fig.10 - Distance r as a function of total pulsed radar delay time

By observing the graph, it is possible to state that for a distance of about 1 m there will be a total delay time of approximately $1{,}077 \times 10^{-8}$ seconds.

D-2.2. Analytical study not knowing the distance to the target from the wall

This study, unlike the previous one, is based on an incident wave between three middle, middle 1 and 3 corresponding to air and middle 2 corresponding to a masonry wall, in which middle 2; in medium 3 is a target whose distance is unknown, for example a person, with $\sigma = 1\ [m^2]$. Note that the middle parameters 1 and 3 (air) are as follows: $\sigma_{1/3} = 0\ [S.m^{-1}]$, $\varepsilon_{1/3} = \frac{10^{-9}}{36\pi}\ [F.m^{-1}]$, $\mu_{1/3} = 4\pi \times 10^{-7}\ [H.m^{-1}]$ and middle 2 are: $\sigma_2 = 0{,}005\ [S.m^{-1}]$, $\varepsilon_2 = 5{,}56\ [F.m^{-1}]$, $\mu_2 = 1\ [H.m^{-1}]$. It is also known that $n_1 = 1$ and $n_2 = \sqrt{5{,}56}$.
Since the distance d_3 (distance from the target vertically) which corresponds to the distance at which the target is from the wall is unknown (Fig. 6), using the MATLAB program it was necessary to apply equations that would help in the calculation of this distance. Thus, the total delay time of the pulsed radar was related, relating it to the incidence angles θ_1, θ_2, θ_3, θ'_1, θ'_2 e θ'_3 (equation 33). The relationships used were as follows:

$$\begin{aligned} n_1 \sin\theta_1 &= n_2 \sin\theta_2 \\ n_1 \sin\theta'_1 &= n_2 \sin\theta'_2 \\ \theta_1 &= \theta_3 \\ \theta'_1 &= \theta'_3 \end{aligned} \quad (34)$$

$$\begin{aligned} r &= d_1 \tan\theta_1 + d_2 \tan\theta_2 + d_3 \tan\theta_3 \\ r' &= d_1 \tan\theta'_1 + d_2 \tan\theta'_2 + d_3 \tan\theta'_3 \end{aligned} \quad (35)$$

Knowing that r and r' have values of 1 m, assuming that a sweep was carried out knowing its value.
Thus, the graph that relates the angles of incidence 1 and 2 as a function of the Total Delay Time was obtained.

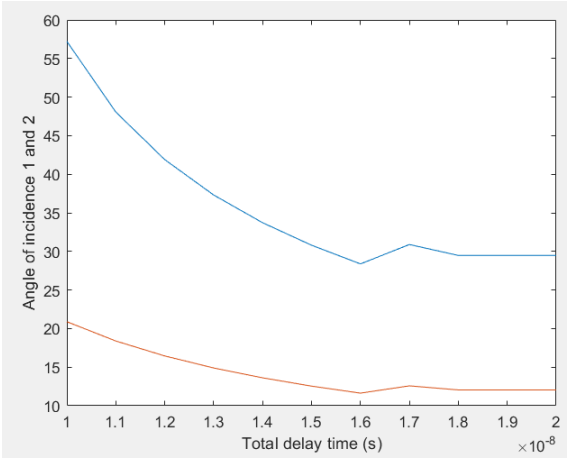

Fig.11 - Incidence angles 1 (blue) and 2 (red) as a function of the total delay time

It was also possible to present a graph representing the distance from the target to the wall, d_3, as a function of the total delay time and a graph of the received Power as a function of the distance from the target to the wall, d_3.

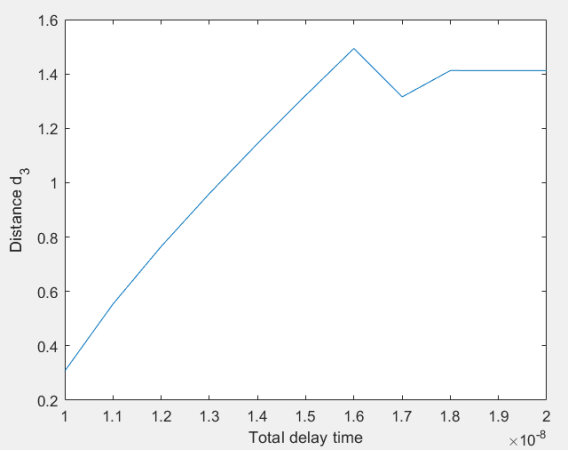

Fig. 12 - Distance d_3 as a function of the total delay time

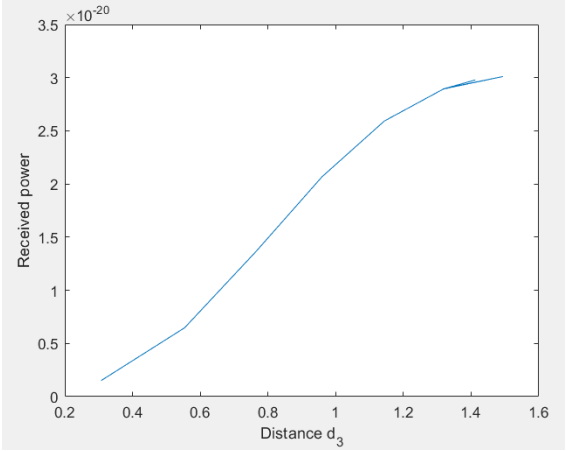

Fig. 13 - Received Power as a function of distance d_3

III. CHARACTERIZATION OF THE WALL

Previously, more specifically in chapter 2, to carry out the calculations, a masonry wall was used with the following electrical permittivity, ε = 5.56 F.m-1, however it should be noted that this type of wall was considered, so the most correct and necessary one to use in the future will be a relative permittivity value that fits each situation. That said, it will be possible to acquire this value in a correct and non-general way, which will be presented below.

A. Electrical permittivity ε

It should be noted that the value of ε is related as follows:

$$\varepsilon = \varepsilon_0 \cdot \varepsilon_r \tag{36}$$

Where ε_0 represents the electrical permittivity in a vacuum with a fixed value of $\frac{10^{-9}}{36\pi}$ F/m, and ε_r represents the relative electrical permittivity. In turn, the value of electrical permittivity depends on the material from which it is made. It is also known that the value of the relative magnetic permeability of the wall has a fixed value of 1. In turn, and according to [2], it is possible to establish an expression that allows calculating the value of the relative electrical permittivity ε_r, which can be expressed and understood as follows:

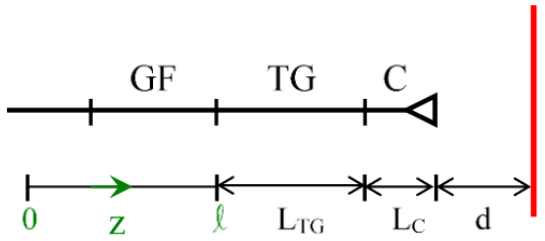

Fig.14 - Measurement of the relative electrical permittivity of materials without a wall [28]

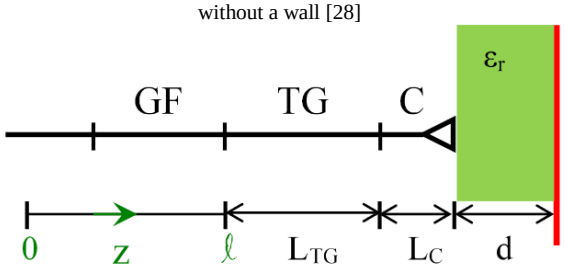

Fig. 15 - Measurement of the relative electrical permittivity of walled materials [28]

Where in both figures GF represents the split guide, TG represents the guide section, C represents the horn, d represents the wall thickness, the red line represents a metal plate, in this case a target, L_{TG} represents the length of the section of guide and L_C represents the length of the horn.
By observing Fig. 14 the following relationships can be established:

$$\begin{aligned} k_{z1}(l - z_{min1}) + k_{z1}L_{TG} + k_{z2}L_C + k_0 d = 0 \\ k_{z1}(l - z_{min2}) + k_{z1}L_{TG} + k_{z2}L_C + k_1 d = 0 \end{aligned} \tag{37}$$

Where $k_1 = k_0\sqrt{\varepsilon_r}$
However, the expression above represents the situation in which there is no wall where z_{min1} represents the minimum distance that the metal plate is from the horn and z_{min2} represents the minimum distance that the metal plate is away from the wall.
Therefore, and using the same reasoning as in the first situation, the same expressions of (37) are applied with small changes and it will be possible to calculate the value of ε_r , as illustrated in Fig. 15.

$$k_{z1}(l - z_{min2}) + k_{z1}L_{TG} + k_{z2}L_C + k_0 d = 0$$
$$k_{z1}(l - z_{min3}) + k_{z1}L_{TG} + k_{z2}L_C + k_1 d = 0 \quad (38)$$

Where z_{min3} represents the minimum distance of the metal plate against the wall and z_{min2} represents the minimum distance of the metal plate against the wall.
The following expression is thus obtained for calculating the relative electrical permittivity of the wall ε_r:

$$\varepsilon_r = \left[1 + \frac{\lambda_0}{\lambda_z}\frac{(z_{min3} - z_{min2})}{d}\right]^2 \quad (39)$$

B. Determination of electrical permittivity in real situation

In this subchapter, the electrical permittivity ε of the wall was calculated. That said, a laboratory assembly was carried out in order to calculate the value of the relative electrical permittivity of the wall ε_r , as can be seen in the figures below:

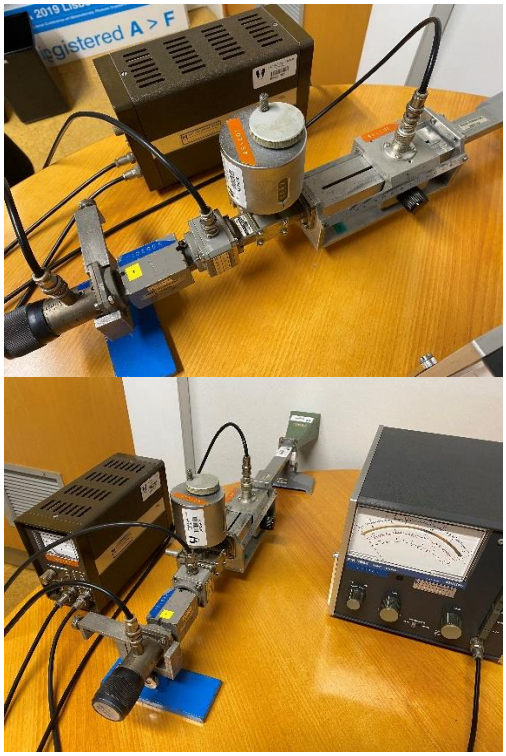

Fig. 16 - Laboratory setup for calculating the relative electrical permittivity of the wall ε_r

The expressions used for the calculation were those presented in subchapter *A*, more specifically equation (39).
The data obtained were the following:
f = 8.945 GHz
a = 22.86 mm
d = 107.3 mm
λ_0 = 33.54 mm
λ_z = 49.35 mm

Metal plate leaning against the horn:

z_{min1}= 39.5 mm
$z_{min1}{}'$ = 89.1 mm

Plate on the other side of the wall:

z_{min3} = 62.5 mm
$z_{min3}{}'$= 111.8 mm
It is known that $z_{min2} = z_{min1} + (d_2 - d_1) \cdot \frac{\lambda_z}{\lambda_0}$, where $d_2 - d_1 = d$, thus obtaining the value of $z_{min2} = 197{,}38mm$.
Applying equation (39), and making $z_{min1} = z_{min2}$ e $z_{min2} = z_{min3}$,we get ε_r= 4.
Thus, and according to equation (36).

IV. VIRTUAL APERTURE RADAR

Virtual Aperture Radar (VAR) can also be defined as a MIMO radar system, since it obtains the image of a region of interest based on MIMO antennas [3]. This consists of a multiple antenna system, in which MIMO stands for Multiple Input Multiple Output. That said, each transmit antenna radiates an arbitrary waveform independently of the other transmit antennas. In turn, each receiving antenna can receive these signals. Thus, an antenna field of N transmitters and a field of K receivers, mathematically, results in a virtual field of K·N elements with an enlarged size of a virtual aperture [4].
This type of radar system is used for numerous purposes, namely the improvement of spatial resolution, by providing a substantially improved immunity to interference. These radars improve the signal/noise ratio, so the probability of target detection also increases [4].

A. Rectification using the Radar cross section of a person

Earlier in chapter 2, more specifically in subchapter *D-2.2* the study of the wave was presented according to the bistatic model in three different ways in which the distance d_3, (distance from the vertical target) was unknown, which corresponds to the distance at which the target is from the wall, however in this study and in the ones previously carried out, the expression of receiving collection out of second an antenna gain value, $G = 16db$, as well as the value of the radar cross section, σ, with a fixed value of $1m^2$, is correct in reality, since incident parameters dependent on the antennas and the reflection of the waves in the antennas both for emission and reception. Thus, if the value of the gain gains of the horn emission antennas, G_1, and the reception antenna G_2 is decomposed and the respective specific incidence and reflection receptions, respectively, θ_1 and θ'_1 , it should be noted that the antennas have the same characteristics so they receive the same gain value ($G = 16db$); and in turn the radar cross section of a person, σ, still from the same angles of

reflection and reflection, respectively, θ_3 and θ'_3. Post this is a correct expression and to adopt was the following:

$$P_r = \frac{P_e \times (G_1 \times \cos\theta_1) \times (G_2 \times \cos\theta'_1) \times \lambda^2 \times (\sigma \times \cos\theta_3 \times \cos\theta'_3)}{(4\pi)^3 (R_1 + R_2 + R_3)^2 (R'_1 + R'_2 + R'_3)^2} \times |T_{TM21}|^2 \times |T_{TM12}|^2 \times |T_{TM23}|^2 \times |T_{TM32}|^2 \times |T_{TM'21}|^2 \times |T_{TM'12}|^2 \times |T_{TM'23}|^2 \times |T_{TM'32}|^2 e^{-4\alpha R_2 R'_2} \quad (40)$$

In turn, the graph representing the received power as a function of distance r is,

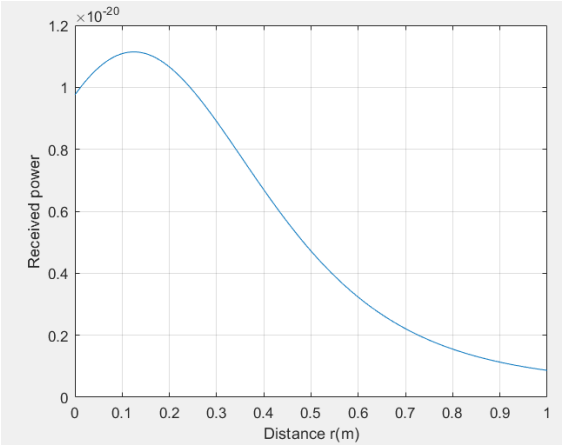

Fig. 17 - Received power as a function of distance r

The graph that represents the general case of the radar cross section of a person, σ, as a function of the angles of incidence and reflection, respectively, θ_3 and θ'_3, is shown below.

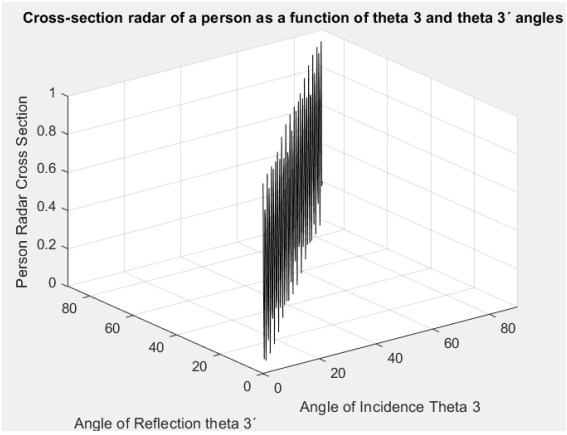

Fig.18 - Radar cross-section of a person, σ, as a function of angles θ_3 and θ'_3

B. Laboratory Measures

This subchapter will present the results of a study carried out in a laboratory environment of a possible real situation, which consisted of measuring the different powers obtained with two antennas, moving them along the wall while on the other side of the wall (behind) the target was found, which instead of being a human target, a metal plate was used. The assembly consisted of placing two pyramidal horn antennas, each with a gain of 15 dB, spaced about 13 cm from each other, with the frequency used being 9 GHz. A metal plate was placed on the other side of the wall, parallel to the two antennas. The wall has a thickness of 10.1 cm, the distance from the plate to the wall was 5.6 cm and the distance from the wall to the antennas as well as the distance between the two antennas varied. It is possible to visualize the implemented assembly in the figures below.

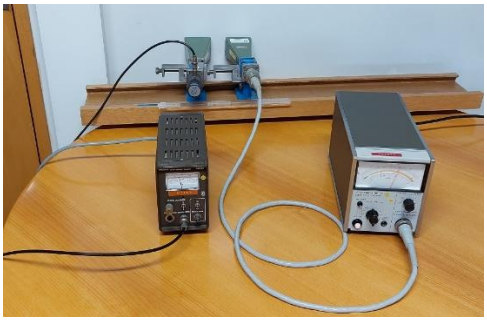

Fig. 19 - Experimental assembly of two pyramidal horn antennas with power supply and a power meter

Fig. 20 - Installing the two pyramidal horn antennas in parallel with the wall

Fig. 21 - Installing the metal plate (target) behind the wall

Several power measurements were performed along a length of 30 cm, which corresponded to the displacement of the antennas. First, measurements were performed with a distance between antennas of 13 cm, just varying the distance between the antennas and the wall. The first measurement was done at a distance of 2mm.
Then measurements were done with the distance from the horns to the wall of 5mm and finally 10mm.
According to the measurements carried out, it was possible to obtain the following graph:

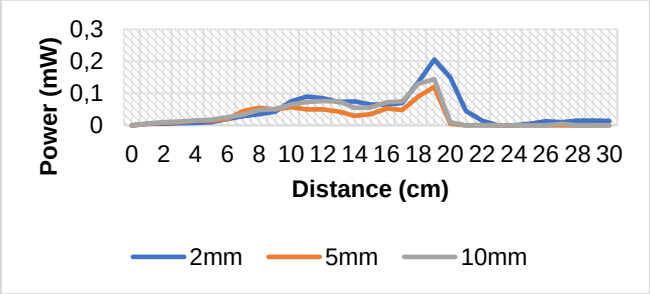

Fig. 22 - Power graph as a function of distance with variation of the distance between the wall and the antennas

By observing the graph, it is possible to verify that there is a peak at 19 cm in all cases, which allows identifying the location of the target, indicating that the antennas are completely parallel to the metallic plate. It is verified that the detection capability improves when the distance to the wall is reduced, as expected [2]
Measurements were also carried out but keeping the distance between the antennas and the wall (2mm) and varying the distance between the two antennas. Measurements were taken at 13cm, 20cm and 7.5cm.
That said, it is possible to graphically visualize the result of these measurements.

[4]

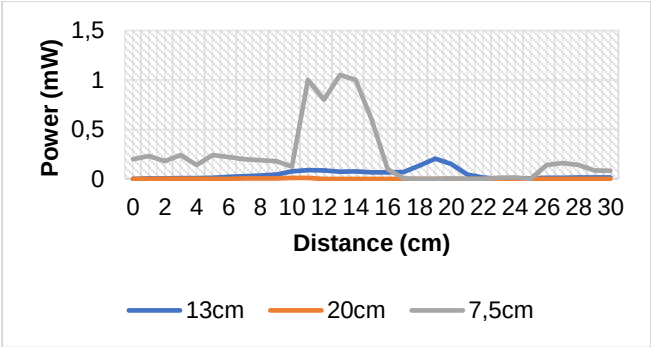

Fig. 23 - Graph of power as a function of distance with variation of the distance between the two antennas

With the observation of the graph, it is possible to affirm that the closer the two antennas are, the greater the received power, and the detection capacity.

V. CONCLUSIONS

The main objective of this work is the study of the use of a virtual aperture radar to obtain an image through the wall. Radar technology has been undergoing changes from an evolutionary and promising point of view, so obtaining radar images through the wall has proved to be an important tool, which can be applicable in the military, police, or in the support of firefighters and civil protection as it allows the detection, location and identification of targets that are behind opaque obstacles, such as a wall.
During the development of this study, it was possible to conclude that in order to obtain an image through the wall, there are numerous aspects to be taken into account, since from the environment to the target and to the obstacle, these have influence and can compromise the good results that are intended. It was also possible to conclude, although the virtual aperture radar presents better results in some aspects compared to another type of radar for obtaining images through the wall, it is still an area to be explored and it is necessary to improve the existing conventional models, namely this type of displayed radar.

REFERENCES

[1] T. Jin and A. Yarovoy, “A Through-the-Wall Radar Imaging Method Based on a Realistic Model”, *International Journal of Antennas and Propagation*, vol. 2015, 2015, doi: 10.1155/2015/539510.

[2] Peixeiro, C. Introdução ao 1º Trabalho de laboratório (Conceitos Fundamentais, Linhas de Transmissão e Guias de Ondas), Propagação e Radiação de Ondas Eletromagnéticas, Instituto Superior Técnico, dezembro 2021.

[3] L. Qiu, Z. Zhou, “Multipath Model and Ghosts Localization in Ultra-Wide Band Virtual Aperture Radar”, College of Electronic Science and Engineering, National University of Defense Technology Changsha 410073, China, 2014.

[4] Christian Wolff. Radar Tutorial - MIMO Radar Systems. url: http://www.radartutorial.
eu/02.basics/MIMO-radar.en.html (acedido em 10 maio 2022).